Extended Abstracts of the 22nd (1990 International) Conference on Solid State Devices and Materials, Sendai, 1990, pp. 1051-1054 **S-E-29**

High Performance a-Si:H TFT Driven Linear Image Sensor with New Multiplex Strucrure for G4 Facsimile

Hiroyuki MIYAKE, Mamoru NOBUE, Kazuhiro SAKAI, Tsutomu ABE*, Yoshihiko SAKAI, Hiroyuki HOTTA, Yasumoto SHIMIZU, Kimio KOIZUMI*, Hisao ITO and Takashi OZAWA

Electronic and Imaging Devices Research Laboratory,
*No.2 Electronic Device Department, Fuji Xerox Co.,Ltd.
2274, Hongo, Ebina-shi, Kanagawa, 243-04, JAPAN

A new 400DPI, A3 page width(310mm) and 4864dot, linear image sensor has been developed on a glass substrate. To achieve high speed and photoresponsivity for G4 facsimile, the sensor has a new parallel multiplex structure called meander lines. The sensor can be driven at 4MHz clock frequency and its photoresponsivity is 20V/lx·s under G54 fluorescent lamp. The reproduced image quality of the sensor is good for 6.5point Kanji characters.

1. Introduction

Page width contact type image sensors have features to reduce the size of image input equipments by using 1:1 focusing optics. Various contact type linear image sensors have been developed, such as multichip CCD sensor[1)], amorphous-silicon(a-Si:H) sensors with a-Si:H thin film transistor(TFT)[2)] or poly-crystalline silicon TFT[3)]. Especially, the image input system for G4 facsimile requires fast speed (less than 1ms/line), fine resolution(400DPI) and high gray scale(more than 64 levels).

We developed a fabrication technology involving the formation of a-Si:H devices on a large glass substrate, and also developed a contact type linear image sensor using a schottky photodiode(PD) which has Cr/a-Si:H/ITO sandwich structure[4)] and a matrix driven image sensor using a-Si:H TFT as a switching device[5)6)]. However in a matrix driven image sensor, crosstalk coupling between the top and bottom signal lines exists, and it decreases the gray scale reading capability. To reduce crosstalk, we made the coupling capacitance smaller and also the line capacitance larger. As the result, a large line capacitance decreased photoresponsivity[7)8)]. In order to solve these problems, we have developed a new wiring structure which connects a group of pixels with the same number of single-layer parallel lines. These multiplex parallel lines are called "meander lines", for their shape look like a meandering river.

2. Device Operation and Equivalent Circuit

According to the equivalent circuit shown in Fig.1, the basic operation is described as follows. Photo-charges generated by light exposure are stored in capacitance of photodiode (C_{PD}:0.5pF), additional capacitance (C_{ADD}: 0.7pF) and parasitic coupling capacitance between gate and drain of TFT (C_{GD}:0.3pF). C_{ADD} is inserted to suppress the feed through due to gate voltage swing. The charges are transferred to line capacitance (C_L) through TFT. The change of signal line voltage is detected by the analog multiplexer. This operation, in other words, is to divide all charges(Q) into all the capacitance($C_{ALL} = C_{PD}+C_{ADD}+C_{GD}+C_{GS}+C_L$) in the circuit. So the capacitance in drain side ($C_{PD}+C_{ADD}+C_{GD}$) and C_L are key parameters to determine the performance, because the photoresponsivity and the after image are related to Q/C_{ALL} and $(C_{PD}+C_{ADD}+C_{GD})/C_{ALL}$, respectively[9)].

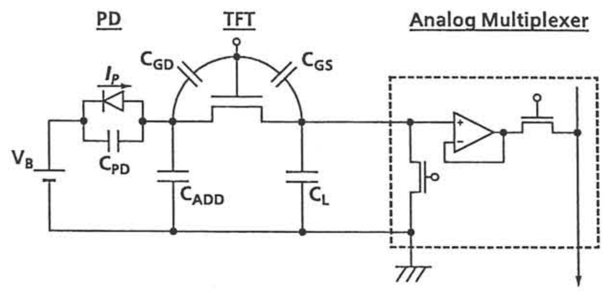

Figure 1. Equivalent circuit of one pixel of the sensor. V_B is bias voltage for PD, C_{PD} is capacitance of PD, C_{ADD} is additional capacitance, C_{GD} and C_{GS} are parasitic coupling capacitance between gate and drain or source of TFT, C_L is line capacitance.

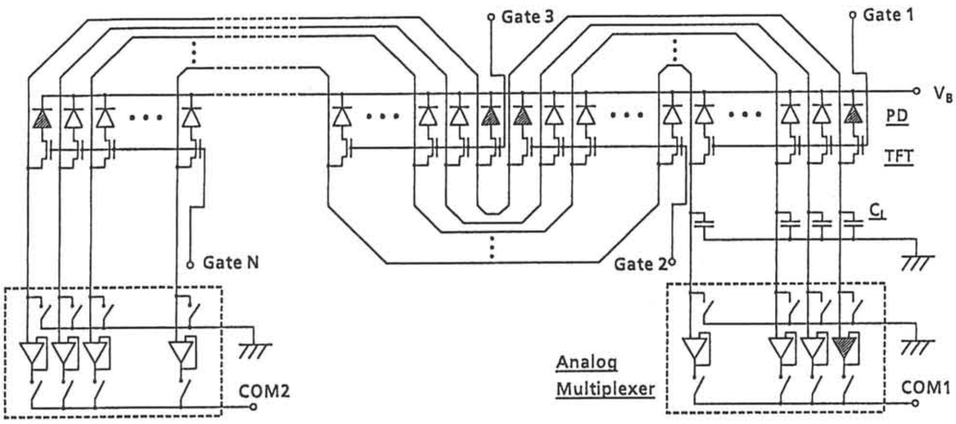

Figure 2. Equivalent circuit of A5 page width sensor with meander lines. Gate driver circuit and ground lines are omitted.

According to the conventional matrix multiplex lines, there is a trade off between reduction of crosstalk and increase of photoresponsivity. That is because the crosstalk is proportion to the ratio of the coupling capacitance to the line capacitance, while the photoresponsivity is inverse proportion to the line capacitance itself. In order to overcome these trade off problems, we introduced the meander multiplex lines.

Figure 2 shows the equivalent circuit of the sensor. It contains the meander lines, the photodiode array and two analog multiplexers. There are no crossover points between signal lines. To suppress the voltage swing affected by the adjacent signal line, a ground line is inserted between every adjacent signal line.

To achieve high speed reading with the 4MHz operating analog multiplexer, two A5 page width subarrays which are mostly same layout are fabricated into line on a glass substrate. This makes double speed reading possible(0.6ms/line) by parallel operation. The C_L on each subarray is less than 1/10 of the conventional matrix lines.

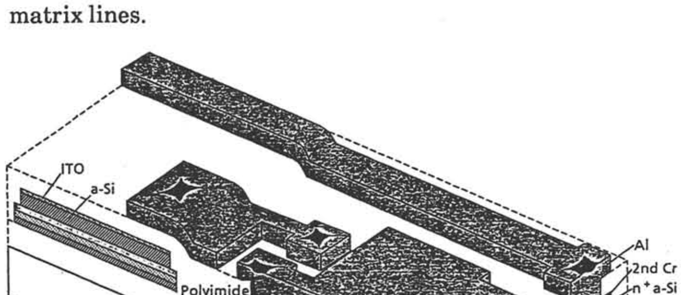

Figure 3. Cross sectional view of a part of the sensor. Passivation layer is omitted. Dark area on aluminum pattern is contact area.

In Fig.2, the stored charges are transferred to C_L by sequential TFT switching of the blocks. Then each signal line voltage is detected and amplified by high speed multiplexer, and serial signal comes out on an output terminal. The output signal sequence in every two blocks must be reversed, because an input signal sequence is led by turns to the input terminals of the multiplexer. To rearrange the signal sequence, two mutiplexers are placed at the both ends of the meander lines and are operated simultaneously. The output signal with proper sequence is obtained by alternately switching of two common outputs from two multiplexers.

3. Device Structure and Fabrication

Figure 3 shows a cross sectional view of the main part of the sensor. It consists of PD, C_{ADD}, TFT and the meander lines. The PD is Cr/a-Si/ITO schottky photodiode with a 63.5μm $\times$ 48.5μm aperture isolated by photolithography. The thickness of a-Si:H is 1.3μm.

The C_{ADD} is composed of metal-insulater-metal-insulater-metal, and the intermediate metal layer is connected to the drain of TFT and others are grounded. All the layers of C_{ADD} are used to compose PD or TFT.

The TFT has an inverted staggered structure. Cr(750Å) and silicon nitride(SiNx, 1500Å) are used as a gate electrode and insulator, respectively. The gate insulator, a-Si:H(500Å) and top-SiNx(1500Å) are deposited successively without breaking vacuum. n+a-Si:H (1000Å) and Cr (1500Å) are used as the source and drain electrodes. W/L of TFT is 180μm /15μm, overlap size of source or drain electrode over gate electrode is 3μm.

Meander lines are aluminum lines (1.5μm) on dielectric layer (polyimide, 1.15μm). Each signal line runs between each PD.

Figure 4 shows a microphotograph of the sensor. The

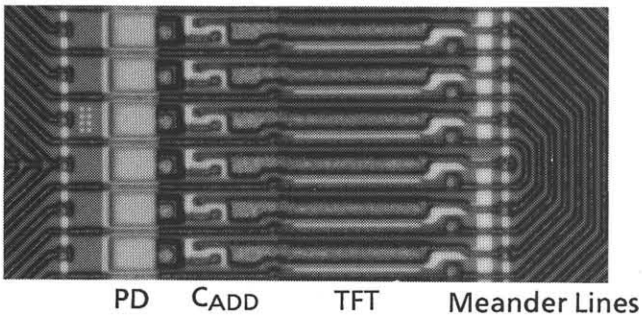

Figure 4. Microphotograph of the sensor.

completed array is mounted on a print circuit board, and connected to the multiplexers by wirebonding.

4. Evaluation of Meander Lines

The width and the space of the meander lines are important parameters to determine the C_L. The vertical line pitch is the same as the pixel pitch. The horizontal pitch is not fixed but required to minimize the array width. If it is wider, the total length of the lines becomes longer, and also C_L becomes larger. The design rule of the horizontal lines is explained, as follows.

Both C_L and the adjacent coupling capacitance(C_C) composed of the aluminum lines are calculated by two-dimentional electric field analysis on a cross section. The adjacent crosstalk is estimated from the ratio of C_C to C_L on each cross section. Figure 5 shows C_L and the adjacent crosstalk as a function of the line width. From this figure, C_L increases moderately as the line width increases, but it decreases more steeply when the space increases. On the

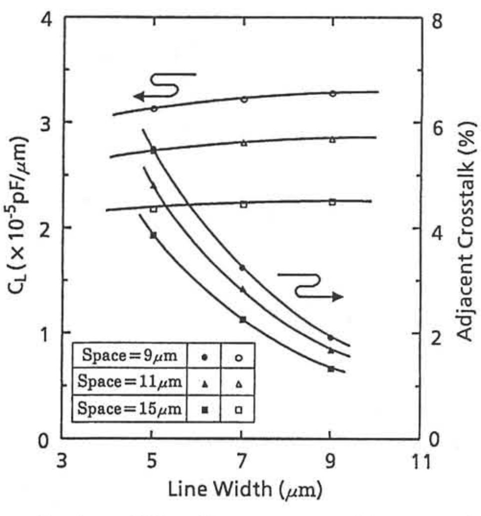

Figure 5. C_L and the adjacent crosstalk versus the line width analyzed by the electric field simulation. The adjacent crosstalk is defined as C_C/C_L.

other hand, the adjacent crosstalk depends on the width rather than the space. But the width and the space are not determined simply. Array width and yield of lines must be considered in determining the width and the space. As the result, 7μm and 11μm for the line width and the space have been adopted.

5. Charge Transfer Characteristics

Figure 6 shows the charge transfer characteristics which indicate the voltage at source electrode of TFT. The photo-charges are transferred to C_L according to the time constant which is determined by both the ON resistance of the TFT and the capacitance on the drain side. In Fig.6(a), linearity under low exposure is good in spite of incomplete transfer because time constant of charge transfer is mostly stable. When gate voltage swings between $\pm$5V, the circuit isn't equilibrium yet at 7.5μsec after TFT switching in Fig.6(b). This means incomplete charge transfer. Its rate is about 10% at the present design. Complete charge transfer will be achieved by increase of gate electric field by both high gate voltage shown in Fig.6(b) or reduction of thickness of gate insulator. However it must be considered to compensate feed through influence.

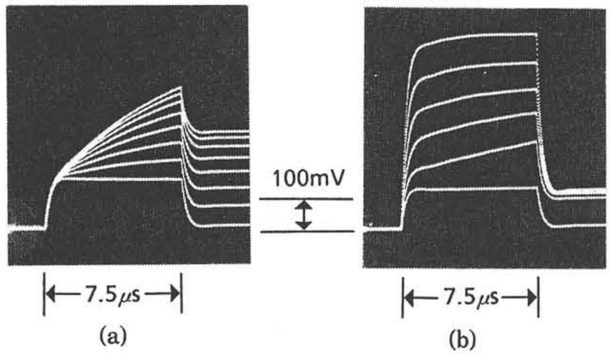

Figure 6. Charge transfer characteristics of the test element. Transfer time is 7.5μsec. (a) Exposed time=0,0.2,0.4,0.6,0.8,1.0,1.2,1.4ms. $V_G=\pm$5V. (b) V_{Gon}=0,2,4,6,8,10V. $V_{Goff}=-5$V.

6. Performance

The light transfer characteristics of the sensor at 4MHz clock frequency is shown in Fig.7. The sensor has good linearity under the low exposure and the reading speed of 0.6ms/line by parallel operation. From this figure, the photoresponsivity is calculated about 20V/lx·s under G54 fluorescent lamp.

As the sensor has the meander lines, crosstalk among each block can be ignored, and adjacent crosstalk which has influence on MTF becomes a problem. Figure 8 shows the adjacent crosstalk characteristics. The influence of the adjacent lines is about 6%, and the next to the adjacent is about 1%. These values are larger than those estimated from the design. The main reason is that the lines are narrower than expected due to larger side etching. Others are that the resistance of the grounded lines might be large, and that relative permittivity of analysis model might be estimated smaller.

Figure 9 shows example of the reproduced image scanned by the sensor. The chart is the facsimile test chart of the Institute of Image Electronics Engineers of Japan. The image was γ-corrected and printed by a sublimation dye thermal transfer. The image quality regarding sharpness and gray levels is good in especially for 6.5 points Kanji characters.

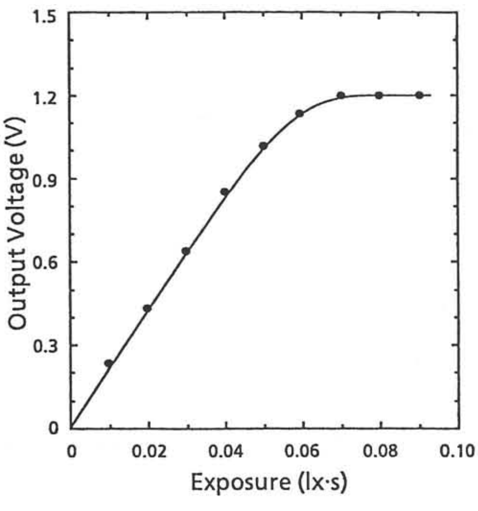

Figure 7. Light transfer characteristics of the sensor operated at 4MHz.

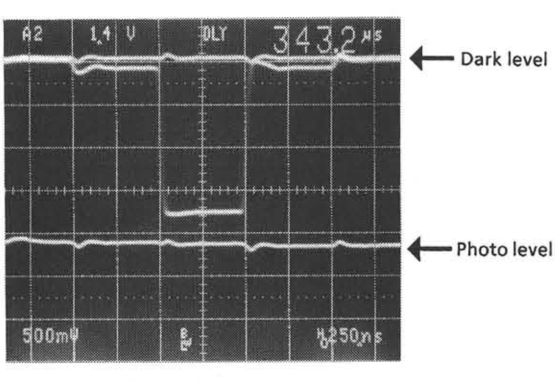

Figure 8. The output of the sensor, when 20μm width light is exposed on only one PD. Horizontal scale: 250ns/div, vertical scale: 0.5v/div.

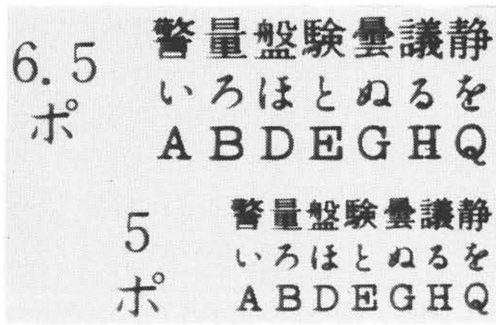

Figure 9. Reproduced image scanned by the sensor.

7. Summary

A new 400DPI, A3 page width linear image sensor has been developed on a glass substrate. The sensor has new parallel multiplex lines called "meander lines" to reduce the crosstalk and C_L. The meander lines were designed, considering both performance and the array size. The sensor can be driven at 4MHz clock frequency and has good linearity under the low exposure. Its photo-responsivity is 20V/lx·s (G54 FL). And the sensor can achieve wide gray scale and fine resolution.

Acknowledgements

The authors would like to express their sincere thanks to the members in Electronic and Imaging Devices Research Laboratory and the members of Suzuka Fuji Xerox for the fabrication of the sensor.

References

1) A.Shudo et al., ITEJ Tech. Rep., 10, (1987) No.52, 7 [in Japanese].
2) F.Okumura et al., Extended Abstracts of the 15th Conf. Solid State Devices and Materials, Tokyo, (1983) p.201.
3) S.Morozumi et al., Extended Abstracts of the 16th Conf. Solid State Devices and Materials, Kobe, (1984) p.559.
4) T.Hamano et al., Proc. 13th Conf. Solid State Devices, Tokyo,1981, Jpn. J. Appl. Phys., 21, (1982) Supple. 21-7, p.245.
5) H.Ito et al., IEDM Dig. Tech. Pap., Washington, (1985) p.436.
6) H.Ito et al., Mat. Res. Soc. Symp. Proc. 95 (1987) p.437.
7) M.Nobue et al., IEICE Tech. Rep., 88, (1989) No.446, 41 [in Japanese].
8) H.Miyake et al., IEICE Tech. Rep., 89, (1990) No.441, 7 [in Japanese].
9) Y.Nishihara et al., J. Non-Cryst. Solids 115 (1989) p.183.